

# Static quark anti-quark interactions in zero and finite temperature QCD. I. Heavy quark free energies, running coupling and quarkonium binding

Olaf Kaczmarek\*

*Fakultät für Physik, Universität Bielefeld, D-33615 Bielefeld, Germany*

Felix Zantow†

*Physics Department, Brookhaven Natl. Laboratory, Upton, New York 11973, USA*

(Dated: December 12, 2019)

We analyze heavy quark free energies in 2-flavor QCD at finite temperature and the corresponding heavy quark potential at zero temperature. Static quark anti-quark sources in color singlet, octet and color averaged channels are used to probe thermal modifications of the medium. The temperature dependence of the running coupling,  $\alpha_{qq}(r, T)$ , is analyzed at short and large distances and is compared to zero temperature as well as quenched calculations. In parts we also compare our results to recent findings in 3-flavor QCD. We find that the characteristic length scale below which the running coupling shows almost no temperature dependence is almost twice as large as the Debye screening radius. Our analysis supports recent findings which suggest that  $\chi_c$  and  $\psi$  are suppressed already at the (pseudo-) critical temperature and thus give a probe for quark gluon plasma production in heavy ion collision experiments, while  $J/\psi$  may survive the transition and will dissolve at higher temperatures.

PACS numbers: 11.15.Ha, 11.10.Wx, 12.38.Mh, 25.75.Nq

## I. INTRODUCTION

The study of the fundamental forces between quarks and gluons is an essential key to the understanding of QCD and the occurrence of different phases which are expected to show up when going from small to high temperatures ( $T$ ) and/or baryon number densities. For instance, at small or vanishing temperatures quarks and gluons get confined by the strong force while at high temperatures asymptotic freedom suggests a quite different QCD medium consisting of rather weakly coupled quarks and gluons, the so-called quark gluon plasma (QGP) [1]. On quite general grounds it is therefore expected that the interactions get modified by temperature. For the analysis of these modifications of the strong forces the change in free energy due to the presence of a static quark anti-quark pair separated by a distance  $r$  in a QCD-like thermal heat bath has often been used since the early work [2, 3]. In fact, the static quark anti-quark free energy which is obtained from Polyakov loop correlation functions calculated at finite temperature plays a similar important role in the discussion of properties of the strong force as the static quark potential does at zero temperature.

The properties of this observable (at  $T = 0$ : potential, at  $T \neq 0$ : free energy) at short and intermediate distances ( $rT \lesssim 1$ ) is important for the understanding of in-medium modifications of heavy quark bound states. A quantitative analysis of heavy quark free energies becomes of considerable importance for the discussion of

possible signals for the quark gluon plasma formation in heavy ion collision experiments [4, 5]. For instance, recent studies of heavy quarkonium systems within potential models use the quark anti-quark free energy to define an appropriate finite temperature potential which is considered in the non-relativistic Schrödinger equation [6, 7, 8, 9]. Such calculations, however, do not quite match the results of direct lattice calculations of the quarkonium dissociation temperatures which have been obtained so far only for the pure gauge theory [10, 11]. It was pointed out [12] that the free energy ( $F$ ) of a static quark anti-quark pair can be separated into two contributions, the internal energy ( $U$ ) and the entropy ( $S$ ). The separation of the entropy contribution from the free energy, *i.e.* the variable  $U = F + TS$ , could define an appropriate effective potential at finite temperature<sup>1</sup> [12, 13],  $V_{\text{eff}}(r, T) \equiv U$ , to be used as input in model calculations and might explain in parts the quantitative differences found when comparing solutions of the Schrödinger equation with direct calculations of spectral functions [10, 11]. First calculations which use the internal energy obtained in our calculations [15, 16, 17, 18] support this expectation. Most of these studies consider so far quenched QCD. Using potentials from the quenched theory, however, will describe the interaction of a heavy quark anti-quark pair in a thermal medium made up of gluons only. It is then important to understand how these results might change for the case of a

---

\*Electronic address: okacz@physik.uni-bielefeld.de

†Electronic address: zantow@quark.phy.bnl.gov

<sup>1</sup> While a definition of the quark anti-quark potential can be given properly at zero temperature using large Wilson loops, at finite temperature a definition of the thermal modification of an appropriate potential energy between the quark anti-quark pair is complicated [14].

thermal heat bath which also contains dynamical quarks.

On the other hand, it is the large distance property of the heavy quark interaction which is important for our understanding of the bulk properties of the QCD plasma phase, *e.g.* the screening property of the quark gluon plasma [19, 20], the equation of state [21, 22] and the order parameter (Polyakov loop) [12, 23, 24, 25]. In all of these studies deviations from perturbative calculations and the ideal gas behavior are expected and were indeed found at temperatures which are only moderately larger than the deconfinement temperature. This calls for quantitative non-perturbative calculations. Also in this case most of todays discussions of the bulk thermodynamic properties of the QGP and its apparent deviations from the ideal gas behavior rely on results obtained in lattice studies of the pure gauge theory, although several qualitative differences are to be expected when taking into account the influence of dynamical fermions; for instance, the phase transition in full QCD will appear as an crossover rather than a 'true' phase transition with related singularities in thermodynamic observables. Moreover, in contrast to a steadily increasing confinement interaction in the quenched QCD theory, in full QCD the strong interaction below deconfinement will show a qualitative different behavior at large quark anti-quark separations. Due to the possibility of pair creation the string-like interaction between the two test quarks can break leading to a constant potential and/or free energy already at temperatures below deconfinement [26].

Thus it is quite important to extend our recently developed concepts for the analysis of the quark anti-quark free energies and internal energies in pure gauge theory [12, 20, 27, 28] to the more complex case of QCD with dynamical quarks, and to quantify the qualitative differences which will show up between pure gauge theories and QCD.

$\beta$	$T/T_c$	# conf.	$\beta$	$T/T_c$	# conf.
3.52	0.76	2000	3.72	1.16	2000
3.55	0.81	3000	3.75	1.23	1000
3.58	0.87	3500	3.80	1.36	1000
3.60	0.90	2000	3.85	1.50	1000
3.63	0.96	3000	3.90	1.65	1000
3.65	1.00	4000	3.95	1.81	1000
3.66	1.02	4000	4.00	1.98	4000
3.68	1.07	3600	4.43	4.01	1600
3.70	1.11	2000			

TABLE I: Sample sizes at each  $\beta$  value and the temperature in units of the (pseudo-) critical temperature  $T_c$ .

For our study of the strong interaction in terms of the quark anti-quark free energies in full QCD lattice configurations were generated for 2-flavor QCD ( $N_f=2$ ) on  $16^3 \times 4$  lattices with bare quark mass  $ma=0.1$ , *i.e.*  $m/T=0.4$ , corresponding to a ratio of pion to rho masses ( $m_\pi/m_\rho$ ) at the (pseudo-) critical temperature of about

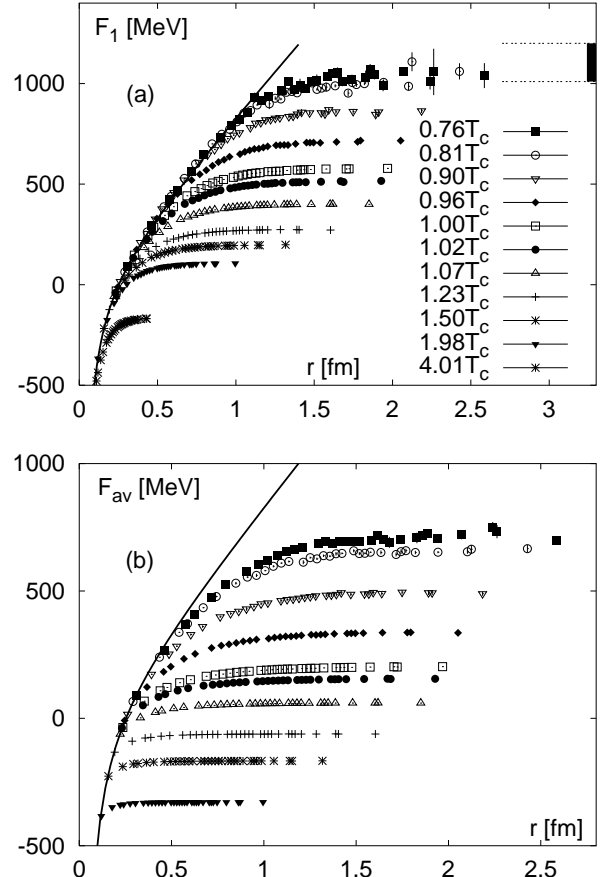


FIG. 1: (a) The color singlet quark anti-quark free energies,  $F_1(r, T)$ , at several temperatures close to the phase transition as function of distance in physical units. Shown are results from lattice studies of 2-flavor QCD. The solid line represents in each figure the  $T = 0$  heavy quark potential,  $V(r)$ . The dashed error band corresponds to the string breaking energy at zero temperature,  $V(r_{\text{breaking}}) \simeq 1000 - 1200$  MeV, based on the estimate of the string breaking distance,  $r_{\text{breaking}} \simeq 1.2 - 1.4$  fm [29]. (b) The color averaged free energy,  $F_{av}(r, T)$ , normalized such that  $F_{av}(r, T) \equiv F_{\bar{q}q}(r, T) - T \ln 9$  [12] approaches the heavy quark potential,  $V(r)$  (line), at the smallest distance available on the lattice. The symbols are chosen as in (a).

0.7 ( $a$  denotes the lattice spacing) [22]. We have used Symanzik improved gauge and p4-improved staggered fermion actions. This combination of lattice actions is known to reduce the lattice cut-off effects in Polyakov loop correlation functions at small quark anti-quark separations seen as an improved restoration of the broken rotational symmetry. For any further details of the simulations with these actions see [30, 31]. In Table I we summarize our simulation parameters, *i.e.* the lattice coupling  $\beta$ , the temperature  $T/T_c$  in units of the pseudo critical temperature and the number of configurations used at each  $\beta$ -value. The pseudo critical coupling for this action is  $\beta_c = 3.649(2)$  [30]. To set the physical

scale we use the string tension,  $\sigma a^2$ , measured in units of the lattice spacing, obtained from the large distance behavior of the heavy quark potential calculated from smeared Wilson loops at zero temperature [22]. This is also used to define the temperature scale and  $a\sqrt{\sigma}$  is used for setting the scale for the free energies and the physical distances. For the conversion to physical units,  $\sqrt{\sigma} = 420$  MeV is used. For instance, we get  $T_c = 202(4)$  MeV calculated from  $T_c/\sqrt{\sigma} = 0.48(1)$  [32]. In parts of our analysis of the quark anti-quark free energies we are also interested in the flavor and finite quark mass dependence. For this reason we also compare our 2-flavor QCD results to the todays available recent findings in quenched ( $N_f=0$ ) [12, 20] and 3-flavor QCD ( $m_\pi/m_\rho \simeq 0.4$  [33]) [34]. Here we use  $T_c = 270$  MeV for quenched and  $T_c = 193$  MeV [34] for the 3-flavor case.

Our results for the color singlet quark anti-quark free energies,  $F_1$ , and color averaged free energies,  $F_{av}$ , are summarized in Fig. 1 as function of distance at several temperatures close to the transition. At distances much smaller than the inverse temperature ( $rT \ll 1$ ) the dominant scale is set by distance and the QCD running coupling will be controlled by the distance. In this limit the thermal modification of the strong interaction will become negligible and the finite temperature free energy will be given by the zero temperature heavy quark potential (solid line). With increasing quark anti-quark separation, however, thermal effects will dominate the behavior of the finite temperature free energies ( $rT \gg 1$ ). Qualitative and quantitative differences between quark anti-quark free energy and internal energy will appear and clarify the important role of the entropy contribution still present in free energies. The quark anti-quark internal energy will provide a different look on the inter-quark interaction and thermal modifications of the finite temperature quark anti-quark potential. Further details of these modifications on the quark anti-quark free and internal energies will be discussed.

This paper is organized as follows: We start in section II with a discussion of the zero temperature heavy quark potential and the coupling. Both will be calculated from 2-flavor lattice QCD simulations. We analyze in section III the thermal modifications on the quark anti-quark free energies and discuss quarkonium binding. Section IV contains our summary and conclusions. A detailed discussion of the quark anti-quark internal energy and entropy will be given separately [35].

## II. THE ZERO TEMPERATURE HEAVY QUARK POTENTIAL AND COUPLING

### A. Heavy quark potential at $T = 0$

For the determination of the heavy quark potential at zero temperature,  $V(r)$ , we have used the measurements of large smeared Wilson loops given in [22] for the same simulation parameters ( $N_f=2$  and  $ma = 0.1$ ) and action.

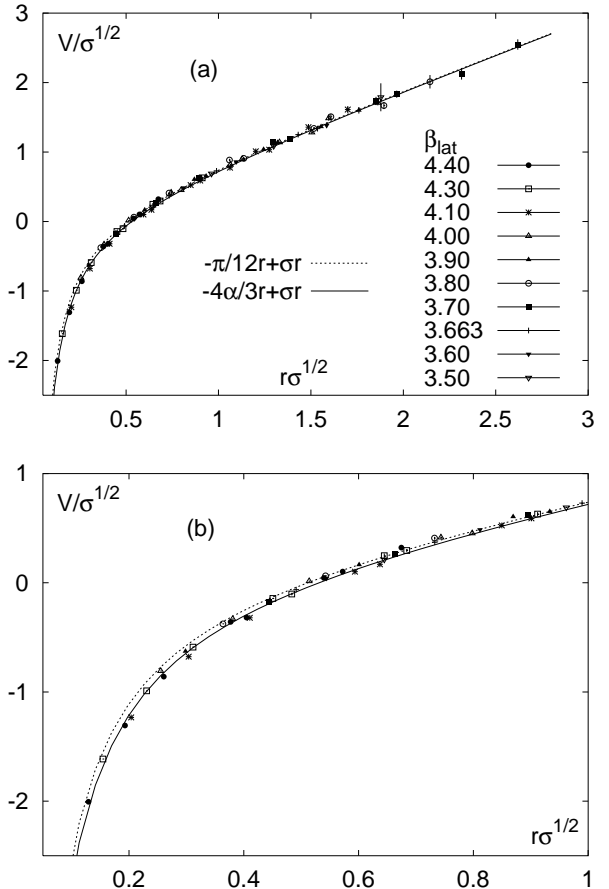


FIG. 2: (a) The heavy quark potential at  $T = 0$  from [22] obtained from 2-flavor QCD lattice simulations with quark masses  $ma = 0.1$  for different values of the lattice coupling  $\beta$ . Fig. 2(b) shows an enlargement of the short distance distance regime. The data are matched to the bosonic string potential (dashed line) at large distances. Included is also the fit to the Cornell form (solid line) given in Eq. (4). Note here that the heavy quark potential from quenched lattice QCD and the string model potential coincide already at  $r\sqrt{\sigma} \gtrsim 0.8$  [36, 37] ( $r \gtrsim 0.4$  fm).

To eliminate the divergent self-energy contributions we matched these data for all  $\beta$ -values (different  $\beta$ -values correspond to different values of the lattice spacing  $a$ ) at large distances to the bosonic string potential,

$$V(r) = -\frac{\pi}{12} \frac{1}{r} + \sigma r \equiv -\frac{4 \alpha_{str}}{3} \frac{1}{r} + \sigma r, \quad (1)$$

where we already have separated the Casimir factor so that  $\alpha_{str} \equiv \pi/16$ . In this normalization any divergent contributions to the lattice potential are eliminated uniquely. In Fig. 2 we show our results together with the heavy quark potential from the string picture (dashed line). One can see that the data are well described by Eq. (1) at large distances, *i.e.*  $r\sqrt{\sigma} \gtrsim 0.8$ , corresponding

to  $r \gtrsim 0.4$  fm. At these distances we see no major difference between the 2-flavor QCD potential obtained from Wilson loops and the quenched QCD potential which can be well parameterized within the string model already for  $r \gtrsim 0.4$  fm [36, 37]. In fact, we also do not see any signal for string breaking in the zero temperature QCD heavy quark potential. This is expected due to the fact that the Wilson loop operator used here for the calculation of the  $T = 0$  potential has only small overlap with states where string breaking occurs [29, 38]. Moreover, the distances for which we analyze the data for the QCD potential are below  $r \lesssim 1.2$  fm at which string breaking is expected to set in at zero temperature and similar quark masses [29].

### B. The coupling at $T = 0$

Deviations from the string model and from the pure gauge potential, however, are clearly expected to become apparent in the 2-flavor QCD potential at small distances and may already be seen from the short distance part in Fig. 2. These deviations are expected to arise from an asymptotic weakening of the QCD coupling, *i.e.*  $\alpha = \alpha(r)$ , and to some extent also is due to the effect of including dynamical quarks, *i.e.* from leading order perturbation theory one expects

$$\alpha(r) \simeq \frac{1}{8\pi} \frac{1}{\beta_0 \log(1/(r\Lambda_{\text{QCD}}))}, \quad (2)$$

with

$$\beta_0 = \frac{33 - 2N_f}{48\pi^2}, \quad (3)$$

where  $N_f$  is the number of flavors and  $\Lambda_{\text{QCD}}$  denotes the corresponding QCD- $\Lambda$ -scale. The data in Fig. 2(b) show a slightly steeper slope at distances below  $r\sqrt{\sigma} \simeq 0.5$  compared to the pure gauge potential given in Ref. [36] indicating that the QCD coupling gets stronger in the entire distance range analyzed here when including dynamical quarks. This is in qualitative agreement with (2). To include the effect of a stronger Coulombic part in the QCD potential we test the Cornell parameterization,

$$\frac{V(r)}{\sqrt{\sigma}} = -\frac{4}{3} \frac{\alpha}{r\sqrt{\sigma}} + r\sqrt{\sigma}, \quad (4)$$

with a free parameter  $\alpha$ . From a best fit analysis of Eq. (4) to the data ranging from  $0.2 \lesssim r\sqrt{\sigma} \lesssim 2.6$  we find

$$\alpha = 0.212(3). \quad (5)$$

This already may indicate that the logarithmic weakening of the coupling with decreasing distance will not too strongly influence the properties of the QCD potential at these distances, *i.e.* at  $r \gtrsim 0.1$  fm. However, the value of  $\alpha$  is moderately larger than  $\alpha_{\text{str}} \simeq 0.196$  introduced

above. To compare the relative size of  $\alpha$  in full QCD to  $\alpha$  in the quenched theory we again have performed a best fit analysis of the quenched zero temperature potential given in [36] using the Ansatz given in Eq. (4) and a similar distance range. Here we find  $\alpha_{\text{quenched}} = 0.195(1)$  which is again smaller than the value for the QCD coupling but quite comparable to  $\alpha_{\text{str}}$ . In earlier studies of the heavy quark potentials in pure gauge theories and full QCD even larger values for the couplings were reported [39, 40, 41, 42, 43, 44]. To avoid here any confusions concerning the value of  $\alpha$  we should stress that  $\alpha$  should not be mixed with some value for the QCD coupling constant  $\alpha_{\text{QCD}}$ , it simply is a fit parameter indicating the 'average strength' of the Coulomb part in the Cornell potential. The QCD coupling could be identified properly only in the entire perturbative distance regime and will be a running coupling, *i.e.*  $\alpha_{\text{qcd}} = \alpha_{\text{qcd}}(r)$ .

When approaching the short distance perturbative regime the Cornell form will overestimate the value of the coupling due to the perturbative logarithmic weakening of the latter,  $\alpha_{\text{QCD}} = \alpha_{\text{QCD}}(r)$ . To analyze the short distance properties of the QCD potential and the coupling in more detail, *i.e.* for  $r \lesssim 0.4$  fm, and to firmly establish here the onset of its perturbative weakening with decreasing distance, it is customary to do so using non-perturbative definitions of running couplings. Following the discussions on the running of the QCD coupling [36, 45, 46, 47, 48], it appears most convenient to study the QCD force, *i.e.*  $dV(r)/dr$ , rather than the QCD potential. In this case one defines the QCD coupling in the so-called  $qq$ -scheme,

$$\alpha_{qq}(r) \equiv \frac{3}{4} r^2 \frac{dV(r)}{dr}. \quad (6)$$

In this scheme any undetermined constant contribution to the heavy quark potential cancels out. Moreover, the large distance, non-perturbative confinement contribution to  $\alpha_{qq}(r)$  is positive and allows for a smooth matching of the perturbative short distance coupling to the non-perturbative large distance confinement signal. In any case, however, in the non-perturbative regime the value of the coupling will depend on the observable used for its definition.

We have calculated the derivatives of the potential with respect to the distance,  $dV(r)/dr$ , by using finite difference approximations for neighboring distances on the lattice for each  $\beta$ -value separately. Our results for  $\alpha_{qq}(r)$  as a function of distance in physical units for 2-flavor QCD are summarized in Fig. 3. The symbols for the  $\beta$ -values are chosen as in Fig. 2(a). We again show in that figure the corresponding line for the Cornell fit (solid line). At large distances,  $r \gtrsim 0.4$  fm, the data clearly mimic the non-perturbative confinement part of the QCD force,  $\alpha_{qq}(r) \simeq 3r^2\sigma/4$ . We also compare our data to the recent high statistics calculation in pure gauge theory (thick solid line) [36]. These data are available for  $r \gtrsim 0.1$  fm and within the statistics of the QCD data no significant differences could be identified between the QCD and pure

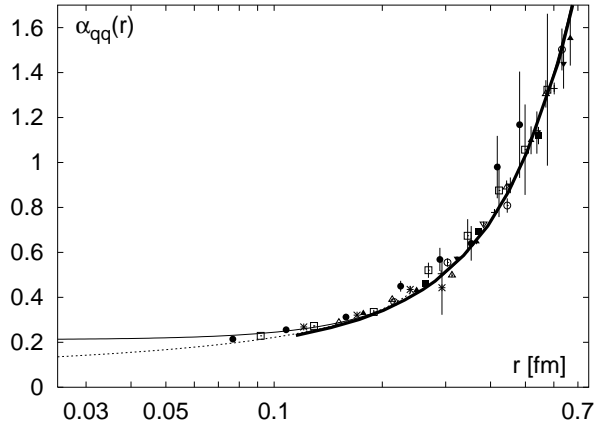


FIG. 3: The short distance part of the running coupling  $\alpha_{qq}(r)$  in 2-flavor QCD at zero temperature defined in Eq. (6) as function of the distance  $r$  (in physical units). The symbols for the different  $\beta$ -values are chosen as indicated in Fig. 2(a). The lines are discussed in the text.

gauge data for  $r \gtrsim 0.4$  fm. At smaller distances ( $r \lesssim 0.4$  fm), however, the data show some enhancement compared to the coupling in quenched QCD. The data below 0.1 fm, moreover, fall below the large distance Cornell fit. This may indicate the logarithmic weakening of the coupling. At smaller distances than 0.1 fm we therefore expect the QCD potential to be influenced by the weakening of the coupling and  $\alpha_{qq}(r)$  will approach values clearly smaller than  $\alpha$  deduced from the Cornell Ansatz. Unfortunately we can, at present, not go to smaller distances to clearly demonstrate this behavior with our data in 2-flavor QCD. Moreover, at small distances cut-off effects may also influence our analysis of the coupling and more detailed studies are required here. Despite these uncertainties, however, in earlier studies of the coupling in pure gauge theory [20, 36, 48] it is shown that the perturbative logarithmic weakening becomes already important at distances smaller than 0.2 fm and contact with perturbation theory could be established.

As most of our lattice data for the finite temperature quark anti-quark free energies do not reach distances smaller than 0.1 fm we use in the following the Cornell form deduced in (4) as reference to the zero temperature heavy quark potential.

### III. QUARK ANTI-QUARK FREE ENERGY

We will analyze here the temperature dependence of the change in free energy due to the presence of a heavy (static) quark anti-quark pair in a 2-flavor QCD heat bath. The static quark sources are described by the Polyakov loop,

$$L(\vec{x}) = \frac{1}{3} \text{Tr}W(\vec{x}), \quad (7)$$

with

$$W(\vec{x}) = \prod_{\tau=1}^{N_\tau} U_0(\vec{x}, \tau), \quad (8)$$

where we already have used the lattice formulation with  $U_0(\vec{x}, \tau) \in SU(3)$  being defined on the lattice link in time direction. The change in free energy due to the presence of the static color sources in color singlet ( $F_1$ ) and color octet ( $F_8$ ) states can be calculated in terms of Polyakov loop correlation functions [3, 49, 50, 51],

$$e^{-F_1(r)/T+C} = \frac{1}{3} \text{Tr} \langle W(\vec{x})W^\dagger(\vec{y}) \rangle, \quad (9)$$

$$e^{-F_8(r)/T+C} = \frac{1}{8} \langle \text{Tr}W(\vec{x})\text{Tr}W^\dagger(\vec{y}) \rangle - \frac{1}{24} \text{Tr} \langle W(\vec{x})W^\dagger(\vec{y}) \rangle, \quad (10)$$

where  $r = |\vec{x} - \vec{y}|$ . As it stands, the correlation functions for the color singlet and octet free energies are gauge dependent quantities and thus gauge fixing is needed to define them properly. Here, we follow [49] and fix to Coulomb gauge. In parts we also consider the so-called color averaged free energy defined through the manifestly gauge independent correlation function of two Polyakov loops,

$$\begin{aligned} e^{-F_{\bar{q}q}(r)/T+C} &= \frac{1}{9} \langle \text{Tr}W(\vec{x})\text{Tr}W^\dagger(0) \rangle \\ &= \langle L(\vec{x})L^\dagger(\vec{y}) \rangle. \end{aligned} \quad (11)$$

The constant  $C$  appearing in (9), (10) and (11) also includes divergent self-energy contributions which require renormalization. Following [12] the free energies have been normalized such that the color singlet free energy approaches the heavy quark potential (solid line) at the smallest distance available on the lattice,  $F_1(r/a = 1, T) = V(r)$ . In Sec. III B we will explain the connection of this procedure to the the renormalized Polyakov loop and show the resulting renormalization constants in Table II.

Some results for the color singlet, octet and averaged quark anti-quark free energies are shown in Fig. 4 for one temperature below and one temperature above deconfinement, respectively. The free energies calculated in different color channels coincide at large distances and clearly show the effects from string breaking below and color screening above deconfinement. The octet free energies above  $T_c$  are repulsive for all distances while below  $T_c$  the distances analyzed here are not small enough to show the (perturbatively) expected repulsive short distance part. Similar results are obtained at all temperatures analyzed here. In the remainder of this section we study in detail the thermal modifications of these free energies from short to large distances. We begin our analysis of the free energies at small distances in Sec. III A with a discussion of the running coupling which leads to the renormalization of the free energies in Sec. III B.

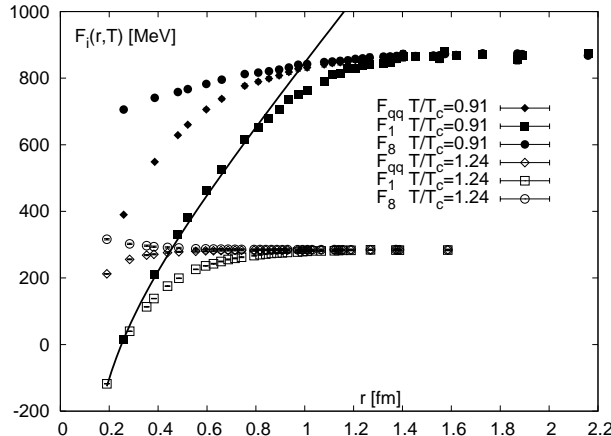


FIG. 4: Heavy quark free energies for 2 flavors of dynamical quarks at a quark mass of  $m/T = 0.4$  calculated on  $16^3 \times 4$  lattices. Shown are the free energies in different color channels, the singlet ( $F_1$ ), octet ( $F_8$ ) and color averaged ( $F_{\bar{q}q}$ ) free energies normalized here as discussed in [12] to the zero temperature potential obtained in Sec. II (solid line).

The separation of small and large distances which characterizes sudden qualitative changes in the free energy will be discussed in Sec. III C. Large distance modifications of the quark anti-quark free energy will be studied in Sec. III D at temperatures above and in Sec. III E at temperatures below deconfinement.

Our analysis of thermal modifications of the strong interaction will mainly be performed for the color singlet free energy. In this case a rather simple Coulombic  $r$ -dependence is suggested by perturbation theory at  $T = 0$  and short distances as well as for large distances at high temperatures. In particular, a proper  $r$ -dependence of  $F_{\bar{q}q}$  is difficult to establish [12]. This maybe is attributed to contributions from higher excited states [52] or to the repulsive contributions from states with static charges fixed in an octet configuration.

### A. The running coupling at $T \neq 0$

We extend here our studies of the coupling at zero temperature to finite temperatures below and above deconfinement following the conceptual approach given in [20]. In this case the appropriate observable is the color singlet quark anti-quark free energy and its derivative. We use the perturbative short and large distance relation from one gluon exchange [3, 50, 51], *i.e.* in the limit  $r\Lambda_{\text{QCD}} \ll 1$  zero temperature perturbation theory suggests

$$F_1(r, T) \equiv V(r) \simeq -\frac{4}{3} \frac{\alpha(r)}{r}, \quad (12)$$

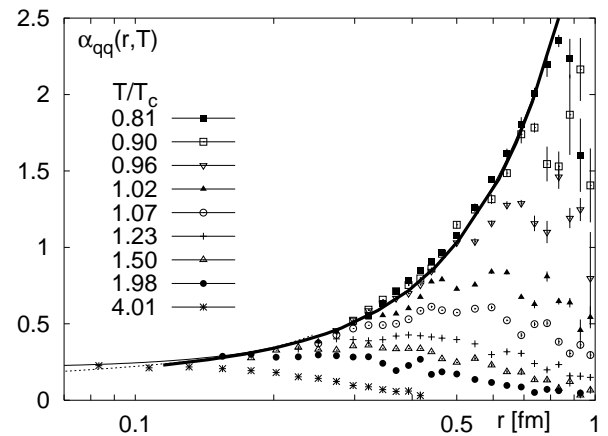


FIG. 5: The running coupling in the  $qq$ -scheme defined in Eq. (14) calculated from derivatives of the color singlet free energies with respect to  $r$  at several temperatures as function of distance below and above deconfinement. We also show the corresponding coupling at zero temperature (solid line) from Eq. (4) and compare the results again to the results in pure gauge theory (thick solid and dashed lines) [36, 48].

while high temperature perturbation theory, *i.e.*  $rT \gg 1$  and  $T$  well above  $T_c$ , yields

$$F_1(r, T) \simeq -\frac{4}{3} \frac{\alpha(T)}{r} e^{-m_D(T)r}. \quad (13)$$

In both relations we have neglected any constant contributions to the free energies which, in particular, at high temperatures will dominate the large distance behavior of the free energies. Moreover, we already anticipated here the running of the couplings with the expected dominant scales  $r$  and  $T$  in both limits. At finite temperature we define the running coupling in analogy to  $T = 0$  as (see [12, 20]),

$$\alpha_{\bar{q}q}(r, T) \equiv \frac{3}{4} r^2 \frac{dF_1(r, T)}{dr}. \quad (14)$$

With this definition any undetermined constant contributions to the free energies are eliminated and the coupling defined here at finite temperature will recover the coupling at zero temperature defined in (6) in the limit of small distances. Therefore  $\alpha_{\bar{q}q}(r, T)$  will show the (zero temperature) weakening in the short distance perturbative regime. In the large distance limit, however, the coupling will be dominated by Eq. (13) and will be suppressed by color screening,  $\alpha_{\bar{q}q}(r, T) \simeq \alpha(T) \exp(-m_D(T)r)$ ,  $rT \gg 1$ . It thus will exhibit a maximum at some intermediate distance. Although in the large distance regime  $\alpha_{\bar{q}q}(r, T)$  will be suppressed by color screening and thus non-perturbative effects will strongly control the value of  $\alpha_{\bar{q}q}(r, T)$ , in this limit the temperature dependence of the coupling,  $\alpha(T)$ , can be extracted by directly comparing the singlet free energy with the high temperature perturbative relation above

deconfinement. Results from such an analysis will be given in Sec. III D.

We calculated the derivative,  $dF_1/dr$ , of the color singlet free energies with respect to distance by using cubic spline approximations of the  $r$ -dependence of the free energies for each temperature. We then performed the derivatives on basis of these splines. Our results for  $\alpha_{qq}(r, T)$  calculated in this way are shown in Fig. 5 and are compared to the coupling at zero temperature discussed already in Sec. II B. Here the thin solid line corresponds to the coupling in the Cornell Ansatz deduced in Eq. (4). We again show in this figure the results from  $SU(3)$ -lattice (thick line) and perturbative (dashed line) calculations at zero temperature from [36, 48]. The strong  $r$ -dependence of the running coupling near  $T_c$  observed already in pure gauge theory [20] is also visible in 2-flavor QCD. Although our data for 2-flavor QCD do not allow for a detailed quantitative analysis of the running coupling at smaller distances, the qualitative behavior is in quite good agreement with the recent quenched results. At large distances the running coupling shows a strong temperature dependence which sets in at shorter separations with increasing temperature. At temperatures close but above  $T_c$ ,  $\alpha_{qq}(r, T)$  coincides with  $\alpha_{qq}(r)$  already at separations  $r \simeq 0.4$  fm and clearly mimics here the confinement part of  $\alpha_{qq}(r)$ . This is also apparent in quenched QCD [20]. Remnants of the confinement part of the QCD force may survive the deconfinement transition and could play an important role for the discussion of non-perturbative aspects of quark anti-quark interactions at temperatures moderately above  $T_c$  [15, 17]. A clear separation of the different effects usually described by the concept of color screening ( $T \gtrsim T_c$ ) and effects usually described by the concept of string-breaking ( $T \lesssim T_c$ ) is difficult to establish at temperatures in the close vicinity of the confinement deconfinement crossover.

We also analyzed the size of the maximum that the running coupling  $\alpha_{qq}(r, T)$  at fixed temperature exhibits at a certain distance,  $r_{max}$ , *i.e.* we identify a temperature dependent coupling,  $\tilde{\alpha}_{qq}(T)$ , defined as

$$\tilde{\alpha}_{qq}(T) \equiv \alpha_{qq}(r_{max}, T). \quad (15)$$

The values for  $r_{max}$  will be discussed in Sec III C (see Fig. 8). Values for  $\tilde{\alpha}_{qq}(T)$  are also available in pure gauge theory [20] at temperatures above deconfinement<sup>2</sup>. Our results for  $\tilde{\alpha}_{qq}(T)$  in 2-flavor QCD and pure gauge theory are shown in Fig. 6 as function of temperature,  $T/T_c$ . At temperatures above deconfinement we cannot identify significant differences between the data from pure gauge and 2-flavor QCD<sup>3</sup>. Only at temperatures quite close but above the phase transition small differences between full

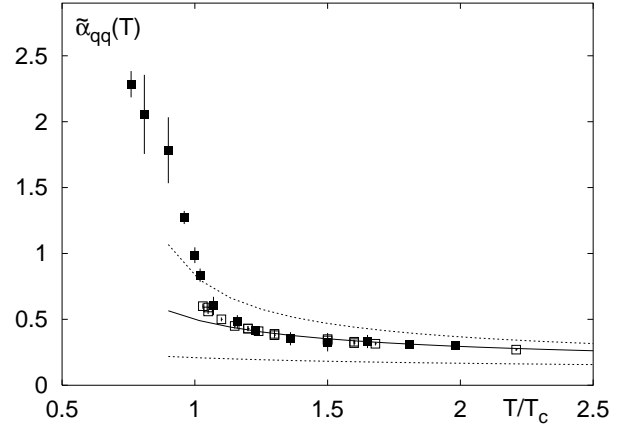


FIG. 6: The size of the maximum,  $\tilde{\alpha}_{qq}(T)$ , defined in Eq. (15), as function of temperature in 2-flavor QCD (filled symbols) and pure gauge theory (open symbols) from [20]. The lines are explained in the text.

and quenched QCD become visible in  $\tilde{\alpha}_{qq}(T)$ . Nonetheless, the value of  $\tilde{\alpha}_{qq}(T)$  drops from about 0.5 at temperatures only moderately larger than the transition temperature,  $T \gtrsim 1.2T_c$ , to a value of about 0.3 at  $2T_c$ . This change in  $\tilde{\alpha}_{qq}(T)$  with temperature calculated in 2-flavor QCD does not appear to be too dramatic and might indeed be described by the 2-loop perturbative coupling,

$$g_{2\text{-loop}}^{-2}(T) = 2\beta_0 \ln\left(\frac{\mu T}{\Lambda_{\overline{MS}}}\right) + \frac{\beta_1}{\beta_0} \ln\left(2 \ln\left(\frac{\mu T}{\Lambda_{\overline{MS}}}\right)\right), \quad (16)$$

with

$$\begin{aligned} \beta_0 &= \frac{1}{16\pi^2} \left( 11 - \frac{2N_f}{3} \right), \\ \beta_1 &= \frac{1}{(16\pi^2)^2} \left( 102 - \frac{38N_f}{3} \right), \end{aligned}$$

assuming vanishing quark masses. In view of the ambiguity in setting the scale in perturbation theory,  $\mu T$ , we performed a best fit analysis to fix the scale for the entire temperature range,  $1.2 \lesssim T/T_c \lesssim 2$ . We find here  $\mu = 1.14(2)\pi$  with  $T_c/\Lambda_{\overline{MS}} = 0.77(21)$  using  $T_c \simeq 202(4)$  MeV [32] and  $\Lambda_{\overline{MS}} \simeq 261(17)$  MeV [53], which is still in agreement with the lower limit of the range of scales one commonly uses to fix perturbative couplings,  $\mu = \pi, \dots, 4\pi$ . This is shown by the solid line (fit) in Fig. 6 including the error band estimated through  $\mu = \pi$  to  $\mu = 4\pi$  and the error on  $T_c/\Lambda_{\overline{MS}}$  (dotted lines). We will turn back to a discussion of the temperature dependence of the coupling above deconfinement in Sec. III D.

At temperatures in the vicinity and below the phase transition temperature,  $T \lesssim 1.2T_c$ , the behavior of  $\tilde{\alpha}_{qq}(T)$  is, however, quite different from the perturbative logarithmic change with temperature. The values

<sup>2</sup> In pure gauge theory  $r_{max}$  and  $\tilde{\alpha}_{qq}(T)$  would be infinite below  $T_c$ .

<sup>3</sup> Note here, however, the change in temperature scale from  $T_c = 202$  MeV in full and  $T_c = 270$  MeV in quenched QCD.

for  $\tilde{\alpha}_{qq}(T)$  rapidly grow here with decreasing temperature and approach non-perturbatively large values. This again shows that  $\tilde{\alpha}_{qq}(r, T)$  mimics the confinement part of the zero temperature force still at relatively large distances and that this behavior persists up to temperatures close but above deconfinement. This again demonstrates the persistence of confinement forces at  $T \gtrsim T_c$  and intermediate distances and demonstrates the difficulty to separate clearly the different effects usually described by color screening and string breaking in the vicinity of the phase transition. We note here, however, that similar to the coupling in quenched QCD [20] the coupling which describes the short distance Coulombic part in the free energies is almost temperature independent in this temperature regime, *i.e.* even at relatively large distances the free energies shown in Fig. 1 show no or only little temperature dependence below deconfinement.

### B. Renormalization of the quark anti-quark free energies and Polyakov loop

On the lattice the expectation value of the Polyakov loop and its correlation functions suffer from linear divergences. This leads to vanishing expectation values in the continuum limit,  $a \rightarrow 0$ , at all temperatures. To become a meaningful physical observable a proper renormalization is required [12, 24, 54]. We follow here the conceptual approach suggested in [12, 28] and extend our earlier studies in pure gauge theory to the present case of 2-flavor QCD. First experiences with this renormalization method in full QCD were already reported in [23, 34].

In the limit of short distances,  $r \ll 1/T$ , thermal modifications of the quark anti-quark free energy become negligible and the running coupling is controlled by distance only. Thus we can fix the free energies at small distances to the heavy quark potential,  $F_1(r \ll 1/T, T) \simeq V(r)$ , and the renormalization group equation (RGE) will lead to

$$\lim_{r \rightarrow 0} T \frac{dF_1(r, T)}{dT} = 0, \quad (17)$$

where we already have assumed that the continuum limit,  $a \rightarrow 0$ , has been taken. On basis of the analysis of the coupling in Sec. III A and experiences with the quark anti-quark free energy in pure gauge theory [12, 20] we assume here that the color singlet free energies in 2-flavor QCD calculated on finite lattices with temporal extent  $N_\tau = 4$  already have approached appropriate small distances,  $r \ll 1/T$ , allowing for renormalization.

The (renormalized) color singlet quark anti-quark free energies,  $F_1(r, T)$ , and the heavy quark potential,  $V(r)$  (line), were already shown in Fig. 1(a) as function of distance at several temperatures close to the phase transition. From that figure it can be seen that the quark anti-quark free energy fixed at small distances approaches finite, temperature dependent plateau values at large distances signaling color screening ( $T \gtrsim T_c$ ) and string

breaking ( $T < T_c$ ). These plateau values,  $F_\infty(T) \equiv F_1(r \rightarrow \infty, T)$ , are decreasing with increasing temperature in the temperature range analyzed here. In general it is expected that  $F_\infty(T)$  will continue to increase at smaller temperature and will smoothly match  $V(r \equiv \infty)$  [6] at zero temperature while it will become negative at high temperature and asymptotically is expected to become proportional to  $g^3 T$  [12, 55]. The plateau value of the quark anti-quark free energy at large distances can be used to define non-perturbatively the renormalized Polyakov loop [12], *i.e.*

$$L^{\text{ren}}(T) = \exp\left(-\frac{F_\infty(T)}{2T}\right). \quad (18)$$

As the unrenormalized free energies approach  $|\langle L \rangle|^2$  at large distances, this may be reinterpreted in terms of a renormalization constant that has been determined by demanding (17) to hold at short distances [25, 56],

$$L^{\text{ren}} \equiv |\langle (Z(g, m))^{N_\tau} L \rangle|. \quad (19)$$

The values for  $Z(g, m)$  for our simulation parameters are summarized in Table II. The normalization constants for the free energies appearing in (9-11) are then given by

$$C = -2N_\tau Z(g, m). \quad (20)$$

An analysis of the renormalized Polyakov loop expectation value in high temperature perturbation theory [55] suggests at (re-summed) leading order<sup>4</sup>, the behavior

$$L^{\text{ren}}(T) \simeq 1 + \frac{2}{3} \frac{m_D(T)}{T} \alpha(T) \quad (21)$$

in the fundamental representation. Thus high temperature perturbation theory suggests that the limiting value at infinite temperature,  $L^{\text{ren}}(T \rightarrow \infty) = 1$  is approached from above. An expansion of (18) then suggests  $F_\infty(T) \simeq -\frac{4}{3}m_D(T)\alpha(T) \simeq -\mathcal{O}(g^3 T)$ . We thus expect  $F_\infty(T) \rightarrow -\infty$  in the high temperature limit.

To avoid here any fit to the complicated  $r$ - and  $T$ -dependence of the quark anti-quark free energy we estimate the value of  $F_\infty(T)$  from the quark anti-quark free energies at the largest separation available on a finite lattice,  $r = N_\sigma/2$ . As the free energies in this renormalization scheme coincide at large distances in the different color channels we determine  $F_\infty(T)$  from the color averaged free energies, *i.e.*  $F_\infty(T) \equiv F_{\bar{q}q}(r = N_\sigma/2, T)$ . This is a manifestly gauge invariant quantity. In Fig. 7

<sup>4</sup> In Ref. [55] the Polyakov loop expectation value is calculated in pure gauge theory and the Debye mass,  $m_D(T)/T = \sqrt{N_c/3}g(T)$ , enters here through the re-summation of the gluon polarization tensor. When changing from pure gauge to full QCD quark loops will contribute to the polarization tensor. In this case re-summation will lead to the Debye mass given in (24). Thus the flavor dependence in Eq. (21) at this level is given only by the Debye mass.

$\beta$	$Z(g, m)$	$T/T_c$	$L^{\text{ren}}(T)$
3.52	1.333(19)	0.76	0.033(2)
3.55	1.351(10)	0.81	0.049(2)
3.60	1.370(08)	0.90	0.093(2)
3.63	1.376(07)	0.96	0.160(3)
3.65	1.376(07)	1.00	0.241(5)
3.66	1.375(06)	1.02	0.290(5)
3.68	1.370(06)	1.07	0.398(7)
3.72	1.374(02)	1.16	0.514(3)
3.75	1.379(02)	1.23	0.575(2)
3.80	1.386(01)	1.36	0.656(2)
3.85	1.390(01)	1.50	0.722(2)
3.90	1.394(01)	1.65	0.779(1)
3.95	1.396(13)	1.81	0.828(3)
4.00	1.397(01)	1.98	0.874(1)
4.43	1.378(01)	4.01	1.108(2)

TABLE II: Renormalization constants,  $Z(g, m)$ , versus  $\beta$  and the renormalized Polyakov loop,  $L^{\text{ren}}$ , versus  $T/T_c$  for 2-flavor QCD with quark mass  $m/T = 0.4$ .

we show the results for  $L^{\text{ren}}$  in 2-flavor QCD (filled symbols) compared to the quenched results (open symbols) obtained in [12]. In quenched QCD  $L^{\text{ren}}$  is zero below  $T_c$  as the quark anti-quark free energy signals permanent confinement, *i.e.*  $F_\infty(T \lesssim T_c) = \infty$  in the infinite volume limit, while it jumps to a finite value just above  $T_c$ . The singularity in the temperature dependence of  $L^{\text{ren}}(T)$  located at  $T_c$  clearly signals the first order phase transition in  $SU(3)$  gauge theory. The renormalized Polyakov loop in 2-flavor QCD, however, is no longer zero below  $T_c$ . Due to string breaking the quark anti-quark free energies approach constant values leading to non-zero values of  $L^{\text{ren}}$ . Although the renormalized Polyakov loop calculated in full QCD is no longer an order parameter for the confinement deconfinement phase transition, it still shows a quite different behavior in the two phases and a clear signal for a qualitative change in the vicinity of the transition. Above deconfinement  $L^{\text{ren}}(T)$  yields finite values also in quenched QCD.

In the temperature range  $1 \lesssim T/T_c \lesssim 2$  we find that in 2-flavor QCD  $L^{\text{ren}}$  lies below the results in quenched QCD. This, however, may change at higher temperatures. The value for  $L^{\text{ren}}$  at  $4T_c$  is larger than unity and we find indication for  $L_{\text{2-flavor}}^{\text{ren}}(4T_c) \gtrsim L_{\text{quenched}}^{\text{ren}}(4T_c)$ . The properties of  $L^{\text{ren}}$ , however, clearly depend on the relative normalization of the quark anti-quark free energies in quenched and full QCD.

### C. Short vs. large distances

Having discussed the quark anti-quark free energies at quite small distances where no or only little temperature effects influence the behavior of the free energies and at

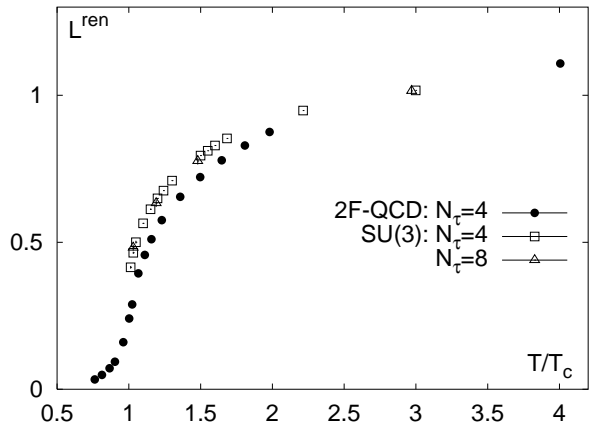


FIG. 7: The renormalized Polyakov loop in 2-flavor QCD (filled circles) compared to the quenched results (open symbols) from [12] as function of temperature in units of the (different) transition temperatures.

quite large distances where aside from  $T$  no other scale controls the free energy, we now turn to a discussion of medium effects at intermediate distances. The aim is to gain insight into distance scales that can be used to quantify at which distances temperature effects in the quark anti-quark free energies set in and may influence the in-medium properties of heavy quark bound states in the quark gluon plasma.

It can be seen from Fig. 1(a) that the color singlet free energy changes rapidly from the Coulomb-like short distance behavior to an almost constant value at large distances. This change reflects the in-medium properties of the heavy quark anti-quark pair, *i.e.* the string-breaking property and color screening. To characterize this rapid onset of in-medium modifications in the free energies we introduced in Ref. [12] a scale,  $r_{\text{med}}$ , defined as the distance at which the value of the  $T = 0$  potential reaches the value  $F_\infty(T)$ , *i.e.*

$$V(r_{\text{med}}) \equiv F_\infty(T). \quad (22)$$

As  $F_\infty(T)$  is a gauge invariant observable this relation provides a non-perturbative, gauge invariant definition of the scale  $r_{\text{med}}$ . While in pure gauge theory the color singlet free energies signal permanent confinement at temperatures below  $T_c$  leading to a proper definition of this scale only above deconfinement, in full QCD it can be deduced in the whole temperature range. On the other hand, the change in the coupling  $\alpha_{qq}(r, T)$  as function of distance at fixed temperature mimics the qualitative change in the interaction when going from small to large distances and the coupling exhibits a maximum at some intermediate distance. The location of this maximum,  $r_{\text{max}}$ , can also be used to identify a scale that characterizes separation between the short distance vacuum-like and the large distance medium modified interaction between the static quarks [20]. Due to the rapid crossover

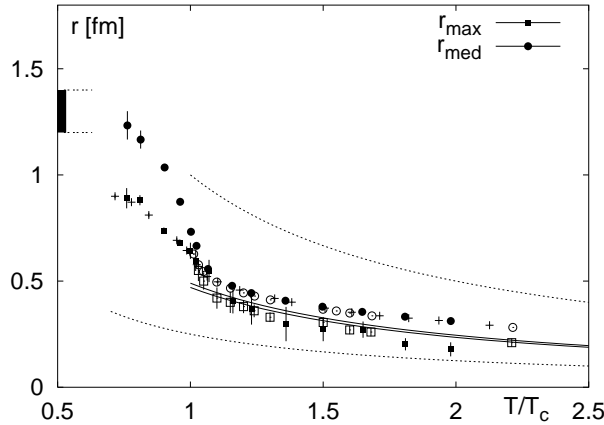


FIG. 8: The location of the maximum in  $\alpha_{qq}(r, T)$  at fixed temperature,  $r_{max}$  ( $N_f=0$ : open squares,  $N_f=2$ : filled squares), and our results for  $r_{med}$  ( $N_f=0$ : open circles,  $N_f=2$ : filled circles,  $N_f=3$ : crosses) defined in Eq. (22) versus  $T/T_c$ . The band at the left frame indicates the distance range at which string breaking is expected to occur in 2-flavor QCD at  $T = 0$  and quark mass  $m_\pi/m_\rho \simeq 0.7$  [29]. The various lines are explained in the text.

from short to large distance behavior (see Fig. 1(a)) it should be obvious that  $r_{med}$  and  $r_{max}$  define similar scales, however, by construction  $r_{max} \lesssim r_{med}$ .

To gain important information about the flavor and quark mass dependence of our analysis of the scales in QCD, we also took data for  $F_\infty(T)$  from Ref. [34] at smaller quark mass,  $m_\pi/m_\rho \simeq 0.4$  [33], and calculated  $r_{med}$  in 3-flavor QCD with respect to the parameterization of  $V(r)$  given in [34]. It is interesting to note here that a study of the flavor and quark mass dependence of  $r_{med}$  and  $r_{max}$  is independent of any undetermined and maybe flavor and/or quark mass dependent overall normalization of the corresponding  $V(r)$  at zero temperature. Our results for  $r_{max}$  ( $N_f=0,2$ ) and  $r_{med}$  ( $N_f=0,2,3$ ) are summarized in Fig. 8 as function of  $T/T_c$ . It can be seen that the value  $r_{max} \simeq 0.6$  fm is approached almost in common in quenched and 2-flavor QCD at the phase transition and it commonly drops to about 0.25 fm at temperatures about  $2T_c$ . No or only little differences between  $r_{max}$  calculated from pure gauge and 2-flavor QCD could be identified at temperatures above deconfinement. The temperature dependence of  $r_{med}$  is similar to that of  $r_{max}$  and again we see no major differences between pure gauge ( $N_f=0$ ) and QCD ( $N_f=2,3$ ) results. In the vicinity of the transition temperature and above both scales almost coincide. In fact, above deconfinement the flavor and finite quark mass dependence of  $r_{med}$  appears quite negligible. At high temperature we expect  $r_{med} \simeq 1/gT$  [12] while in terms of  $r_{max}$  we found agreement with  $r_{max} = 0.48(1)$  fm  $T_c/T$  (solid lines) at temperatures ranging up to  $12T_c$  [20]. Note that both scales clearly lie well above the smallest distance attainable by us on the lattice,  $rT \equiv 1/N_\tau = 1/4$ . This distance is shown by the

lower dashed line in Fig. 8.

At temperatures below deconfinement  $r_{max}$  and  $r_{med}$  rapidly increase and fall apart when going to smaller temperatures. In fact, at temperatures below deconfinement we clearly see difference between  $r_{med}$  calculated in 2- and 3-flavor QCD. To some extend this is expected due to the smaller quark mass used in the 3-flavor QCD study as the string breaking energy gets reduced. It is, however, difficult to clearly separate here a finite quark mass effect from flavor dependence. In both cases  $r_{med}$  approaches, already at  $T \simeq 0.8T_c$ , quite similar values to those reported for the distance where string breaking at  $T = 0$  is expected at similar quark masses. In 2-flavor QCD at  $T = 0$  and quark mass  $m_\pi/m_\rho \simeq 0.7$  the string is expected to break at about  $1.2 - 1.4$  fm [29] while at smaller quark mass,  $m_\pi/m_\rho \simeq 0.4$  it might break earlier [38].

In contrast to the complicated  $r$ - and  $T$ -dependence of the free energy at intermediate distances high temperature perturbation theory suggests a color screened Coulomb behavior for the singlet free energy at large distances. To analyze this in more detail we show in Fig. 9 the subtracted free energies,  $r(F_1(\infty, T) - F_1(r, T))$ . It can be seen that this quantity indeed decays exponentially at large distances,  $rT \gtrsim 1$ . This allows us to study the temperature dependence of the parameters  $\alpha(T)$  and  $m_D(T)$  given in Eq. (13). At intermediate and small distances, however, deviations from this behavior are expected and can clearly be seen and are to some extent due to the onset of the  $r$ -dependence of the coupling at small distances. These deviations from the simple exponential decay become important already below some characteristic scale,  $r_d$ , which we can roughly identify here as  $r_d T \simeq 0.8 - 1$ . This scale which defines a lower limit for the applicability of high temperature perturbation theory is shown by the upper dashed line in Fig. 8 ( $r_d T = 1$ ). It lies well above the scales  $r_{med}$  and  $r_{max}$  which characterize the onset of medium modifications on the quark anti-quark free energy.

#### D. Screening properties above deconfinement and the coupling

##### 1. Screening properties and quarkonium binding

We follow here the approach commonly used [20, 57, 58] and define the non-perturbative screening mass,  $m_D(T)$ , and the temperature dependent coupling,  $\alpha(T)$ , from the exponential fall-off of the color singlet free energies at large distances,  $rT \gtrsim 0.8 - 1$ . A consistent definition of screening masses, however, is accompanied by a proper definition of the temperature dependent coupling and only at sufficiently high temperatures contact with perturbation theory is expected [20, 59]. A similar discussion of the color averaged quark anti-quark free energy is given in Refs. [19, 60, 61].

We used the Ansatz 13 to perform a best-fit analysis of

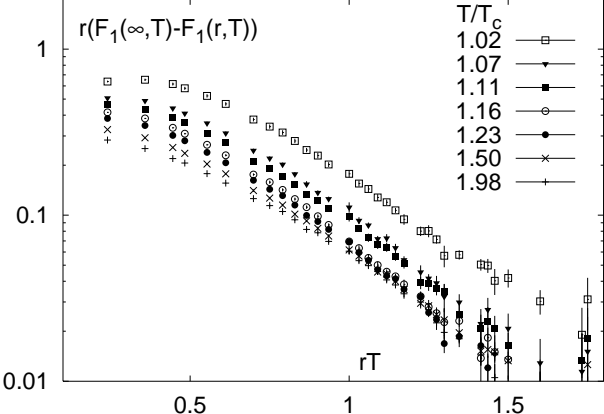


FIG. 9: The color singlet free energy versus  $rT$  obtained from lattice calculations in 2-flavor QCD at several temperatures above deconfinement.

the large distance part of the color singlet free energies, *i.e.* we used fit functions with the Ansatz

$$F_1(r, T) - F_1(r = \infty, T) = -\frac{4a(T)}{3r} e^{-m(T)r}, \quad (23)$$

where the two parameters  $a(T)$  and  $m(T)$  are used to estimate the coupling  $\alpha(T)$  and the Debye mass  $m_D(T)$ , respectively. The fit-range was chosen with respect to our discussion in Sec. III C, *i.e.*  $rT \gtrsim 0.8 - 1$ , where we varied the lower fit limit within this range and averaged over the resulting values. The temperature dependent coupling  $\alpha(T)$  defined here will be discussed later. Our results for the screening mass,  $m_D(T)/T$ , are summarized in Fig. 10 as function of  $T/T_c$  and are compared to the results obtained in pure gauge theory [20]. The data obtained from our 2-flavor QCD calculations are somewhat larger than in quenched QCD. Although we are not expecting perturbation theory to hold at these small temperatures, this enhancement is in qualitative agreement with leading order perturbation theory, *i.e.*

$$\frac{m_D(T)}{T} = \left(1 + \frac{N_f}{6}\right)^{1/2} g(T). \quad (24)$$

However, using the 2-loop formula (16) to estimate the temperature dependence of the coupling leads to significantly smaller values for  $m_D/T$  even when setting the scale by  $\mu = \pi$  which commonly is used as an upper bound for the perturbative coupling. We therefore follow [19, 20] and introduce a multiplicative constant,  $A$ , *i.e.* we allow for a non-perturbative correction defined as

$$\frac{m_D(T)}{T} \equiv A \left(1 + \frac{N_f}{6}\right)^{1/2} g_{2-loop}(T), \quad (25)$$

and fix this constant by best agreement with the non-perturbative data for  $m_D(T)/T$  at temperatures  $T \gtrsim 1.2$ . Here the scale in the perturbative coupling is fixed by

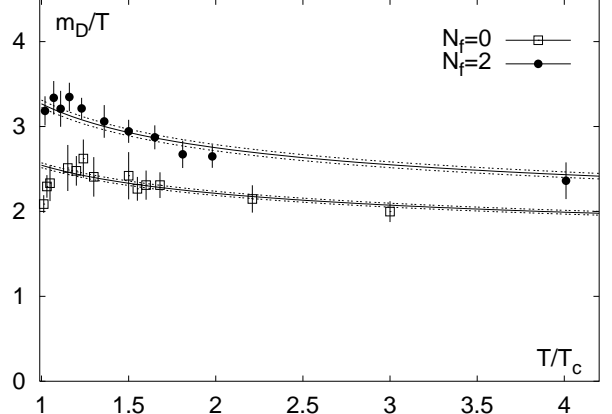


FIG. 10: The non-perturbatively defined screening masses from the large distance behavior of  $F_1(r, T)$  calculated using  $16^3 \times 4$  lattices as function of temperature in 2-flavor QCD (filled circles) and in pure gauge theory (open squares [20]) using  $32^3 \times 4$  lattices. The solid lines show the fit given in Eq. (23) with the corresponding error band (dotted lines).

$\mu = 2\pi$ . This analysis leads to  $A = 1.417(19)$  and is shown as solid line with error band (dotted lines). Similar results were already reported in [19, 20] for screening masses in pure gauge theory. Using the same fit range, *i.e.*  $T = 1.2T_c - 4.1T_c$ , for the quenched results, we obtain  $A = 1.515(17)$ . To avoid here any confusion concerning  $A$  we note that its value will crucially depend on the temperature range used to determine it. When approaching the perturbative high temperature limit,  $A \rightarrow 1$  is expected.

It is interesting to note here that the difference in  $m_D/T$  apparent in Fig. 10 between 2-flavor QCD and pure gauge theory disappears when converting  $m_D(T)$  to physical units. This is obvious from Fig. 11 which shows the Debye screening radius,  $r_D \equiv 1/m_D$ . In general  $r_D$  is used to characterize the distance at which medium modifications of the quark anti-quark interaction become dominant. It often is used to describe the screening effects in phenomenological inter-quark potentials at high temperatures. From perturbation theory one expects that the screening radius will drop like  $1/gT$ . A definition of a screening radius, however, will again depend on the ambiguities present in the non-perturbative definition of a screening mass,  $m_D(T)$ . A different quantity that characterizes the onset of medium effects,  $r_{med}$ , has already been introduced in Sec. III C; this quantity is also expected to drop like  $1/(gT)$  at high temperatures and could be considered to give an upper limit for the screening radius [20]. In Fig. 11 we compare both length scales as function of temperature,  $T/T_c$ , and compare them to the findings in quenched QCD [12, 20]. It can be seen that in the temperature range analyzed here  $r_D(T) < r_{med}(T)$  and no or only little differences between the results from quenched ( $N_f=0$ ) and full ( $N_f=2,3$ ) QCD could be identified. Again we stress that

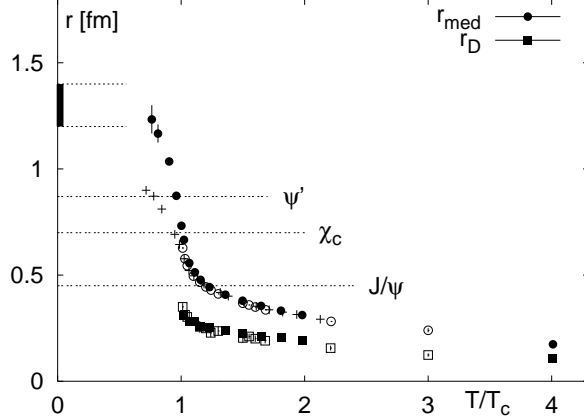


FIG. 11: The screening radius estimated from the inverse Debye mass,  $r_D \equiv 1/m_D$  ( $N_f=0$ : open squares,  $N_f=2$  filled squares), and the scale  $r_{med}$  ( $N_f=0$ : open circles,  $N_f=2$ : filled circles,  $N_f=3$ : crosses) defined in (22) as function of  $T/T_c$ . The dotted line indicates the smallest separation available on lattices with temporal extent  $N_\tau = 4$ . The horizontal lines give the mean squared charge radii of some charmonium states,  $J/\psi$ ,  $\chi_c$  and  $\psi'$  (see also [14]) and the band at the left frame shows the distance at which string breaking is expected in 2-flavor QCD at  $T = 0$  and quark mass  $m_\pi/m_\rho \simeq 0.7$  [29].

in the perturbative high temperature limit differences are expected to arise as expressed by Eq. (24).

It is important to realize that at distances well below  $r_{med}$  medium effects become suppressed and the color singlet free energy almost coincides with the zero temperature heavy quark potential (see Fig. 1(a)). In particular, the screening radius estimated from the inverse Debye mass corresponds to distances which are only moderately larger than the smallest distance available in our calculations (compare with the lower dotted line in Fig. 8). In view of the almost temperature independent behavior of the color singlet free energies at small distances (Fig. 1(a)) it could be misleading to quantify the dominant screening length of the medium in terms of  $r_D \equiv 1/m_D$ . On the other hand the color averaged free energies show already strong temperature dependence at distances similar to  $r_D$  (see Fig. 1(b)).

Following [14] we also included in Fig. 11 the mean charge radii of the most prominent charmonium states,  $J/\psi$ ,  $\chi_c$  and  $\psi'$ , as horizontal lines. These lines characterize the averaged separation  $r$  which enters the effective potential in potential model calculations. It thus is reasonable to expect that the temperature at which these radii equal  $r_{med}$  could give a rough estimate for the onset of thermal effects in the charmonium states. It appears quite reasonable from this view that  $J/\psi$  indeed may survive the phase transition [10, 11], while  $\chi_c$  and  $\psi'$  are supposed to show significant thermal modifications at temperatures close to the transition. Recent potential model calculations support this analysis [16]. The wave functions for these states, however, will also

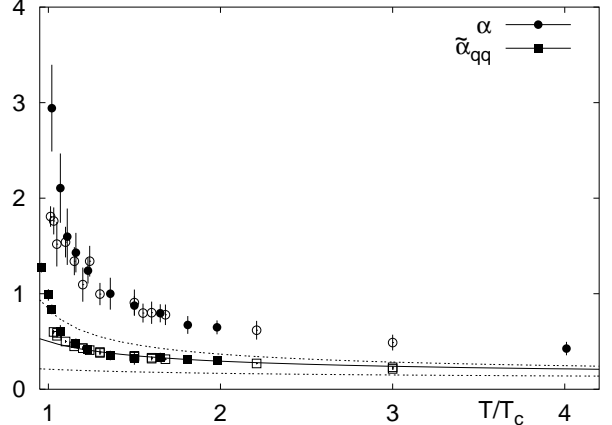


FIG. 12: The temperature dependence of the coupling  $\alpha(T)$  as function of temperature (filled circles) from fits of the large distance behavior of free energies using Eq. (23). We also show again the values of  $\tilde{\alpha}_{qq}(T)$  defined as the maximum value of the running coupling  $\alpha_{qq}(r, T)$  (filled squares) discussed in Sec. III A and the perturbative 2-loop coupling, Eq. (16), with scales  $\mu = \pi, \dots, 4\pi$  (dashed lines). The open symbols indicate results from corresponding quenched QCD calculations [20].

reach out to larger distances [62] and this estimate can only be taken as a first indication for the relevant temperatures. Further details on this issue including also bottomonium states have been given in Ref. [14]. We will turn again to a discussion of thermal modifications of quarkonium states in Ref. [35] using finite temperature quark anti-quark energies.

## 2. Temperature dependence of $\alpha_s$

We finally discuss here the temperature dependence of the QCD coupling,  $\alpha(T)$ , extracted from the fits used to determine also  $m_D$ , *i.e.* from Eq. (23). From fits of the free energies above deconfinement we find the values shown in Fig. 12 as function of  $T/T_c$  given by the filled circles. We again show in this figure also the temperature dependent coupling  $\tilde{\alpha}_{qq}(T)$  introduced in Sec. III A. It can clearly be seen that the values for both couplings are quite different,  $\tilde{\alpha}_{qq}(T) \gtrsim \alpha(T)$ , at temperatures close but above deconfinement while this difference rapidly decreases with increasing temperature. This again demonstrates the ambiguity in defining the coupling in the non-perturbative temperature range due to the different non-perturbative contributions to the observable used for its definition [20]. In fact, at temperatures close to the phase transition temperature we find quite large values for  $\alpha(T)$ , *i.e.*  $\alpha(T) \simeq 2 - 3$  in the vicinity of  $T_c$ , while it drops rapidly to values smaller than unity, *i.e.*  $\alpha(T) \lesssim 1$  already at temperatures  $T/T_c \gtrsim 1.5$ . A similar behavior was also found in [20] for the coupling in pure gauge theory (open symbols). In fact, no or only a marginal enhancement of the values calculated in full QCD com-

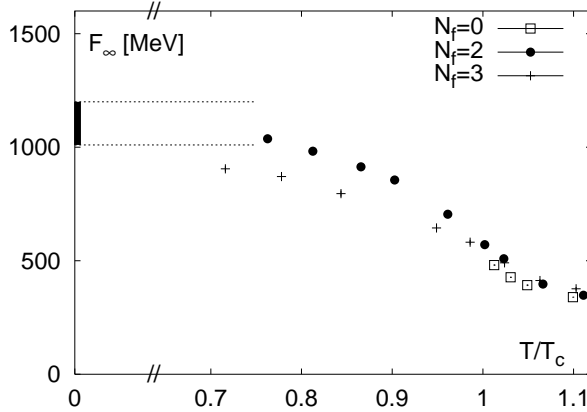


FIG. 13: The plateau value of the quark anti-quark free energy,  $F_\infty(T)$ , calculated in 2-flavor QCD as function of  $T/T_c$  at temperatures in the vicinity and below the phase transition. The dashed lines show the expected value at zero temperature,  $V(r_{\text{breaking}})$ , with  $r_{\text{breaking}} \simeq 1.2 \sim 1.4$  fm using quark mass  $m_\pi/m_\rho \simeq 0.7$  [29]. The open symbols ( $T \gtrsim T_c$ ) correspond to  $F_\infty(T)$  in quenched QCD (from Ref. [12]) and the crosses to 3-flavor QCD studies (from [34]). The relative normalization of the corresponding  $V(r)$  used for renormalization of  $F_1(r \rightarrow \infty, T)$  in quenched and full QCD is such that the Cornell parameterization of  $V(r)$  does not contain any constant at large distances.

pared to the values in quenched QCD could be identified here at temperatures  $T \lesssim 1.5T_c$ . We stress again that the large values for  $\alpha(T)$  found here should not be confused with the coupling that characterizes the short distance Coulomb part of  $F_1(r, T)$ . The latter is almost temperature independent at small distances and can to some extent be described by the zero temperature coupling.

### E. String breaking below deconfinement

We finally discuss the large distance properties of the free energies below  $T_c$ . In contrast to the quark anti-quark free energy in quenched QCD where the string between the quark anti-quark pair cannot break and the free energies are linearly rising at large separations, in full QCD the string between two static color charges can break due to the possibility of spontaneously generating  $q\bar{q}$ -pairs from the vacuum. Therefore the quark anti-quark free energy reaches a constant value also below  $T_c$ . In Fig. 1 this behavior is clearly seen.

The distances at which the quark anti-quark free energies approach an almost constant value move to smaller separations at higher temperatures. This can also be seen from the temperature dependence of  $r_{\text{med}}$  in Fig. 8 at temperature below  $T_c$ . By construction  $r_{\text{med}}$  describes a distance which can be used to estimate a lower limit for the distance where the string breaking will set in. An estimate of the string breaking radius at  $T = 0$

can be calculated from the lightest heavy-light meson,  $r_{\text{breaking}} \simeq 1.2 - 1.4$  fm [29] and is shown on the left side in Fig. 8 within the dotted band. It can be seen that  $r_{\text{med}}$  in 2-flavor QCD does indeed approach such values at temperatures  $T \lesssim 0.8T_c$ . This suggests that the dependence on temperature in 2-flavor QCD is small below the smallest temperature analyzed here,  $0.76T_c$ . This can also be seen from the behavior of  $F_\infty(T)$  shown in Fig. 13 (see also Fig. 1(a)) compared to the value commonly expected at  $T = 0$ . We use  $V(r_{\text{breaking}}) \simeq 1000 - 1200$  MeV as reference to the zero temperature string breaking energy with quark mass  $m_\pi/m_\rho \simeq 0.7$ . This estimate is shown on the left side in Fig. 13 as the dotted band. A similar behavior is expected for the free energies in 3-flavor QCD and smaller quark mass,  $m_\pi/m_\rho \simeq 0.4$ . As seen also in Fig. 13 the values for  $F_\infty(T)$  are smaller than in 2-flavor QCD and larger quark mass. This may indicate that string breaking sets in at smaller distances for smaller quark masses. However, in [22] no mass dependence (in the color averaged free energies) was observed below the quark mass analyzed by us ( $m/T=0.4$ ). At present it is, however, difficult to judge whether the differences seen for 2- and 3-flavor QCD for  $T/T_c < 1$  are due to quark mass or flavor dependence of the string breaking. Although  $F_\infty(T)$  still is close to  $V(r_{\text{breaking}})$  at  $T \sim 0.8T_c$ , it rapidly drops to about half of this value in the vicinity of the phase transition,  $F_\infty(T_c) \simeq 575$  MeV. This value is almost the same in 2- and 3-flavor QCD; we find  $F_\infty^{N_f=2}(T_c) \simeq 575(15)$  MeV and  $F_\infty^{N_f=3}(T_c) \simeq 548(20)$  MeV. It is interesting to note that also the values of  $F_\infty(T)$  in quenched QCD ( $N_f=0$ ) approach a similar value at temperatures just above  $T_c$ . We find  $F_\infty(T_c^+) \simeq 481(4)$  MeV where  $T_c^+ \equiv 1.02T_c$  denotes the closest temperature above  $T_c$  analyzed in quenched QCD. Of course, the value for  $F_\infty(T_c^+)$  will increase when going to temperatures even closer to  $T_c$ . The flavor and quark mass dependence of  $F_\infty(T)$  including also higher temperatures will be discussed in more detail in Ref. [35].

## IV. SUMMARY AND CONCLUSIONS

Our analysis of the zero temperature heavy quark potential,  $V(r)$ , calculated in 2-flavor lattice QCD using large Wilson loops [22] shows no signal for string breaking at distances below 1.3 fm. This is quite consistent with earlier findings [29, 38]. The  $r$ -dependence of  $V(r)$  becomes comparable to the potential from the bosonic string picture already at distances larger than 0.4 fm. Similar findings have also been reported in lattice studies of the potential in quenched QCD [36, 37]. At those distances,  $0.4 \text{ fm} \lesssim r \lesssim 1.5 \text{ fm}$ , we find no or only little differences between lattice data for the potential in quenched ( $N_f=0$ ) given in Ref. [36] and full ( $N_f=2$ ) QCD. At smaller distances, however, deviations from the large distance Coulomb term predicted by the string picture,  $\alpha_{\text{str}} \simeq 0.196$ , are found here when performing best fit analysis with a free Cornell Ansatz. We

find  $\alpha \simeq 0.212(3)$  which could describe the data down to  $r \gtrsim 0.1$  fm. By analyzing the coupling in the  $qq$ -scheme defined through the force,  $dV(r)/dr$ , small enhancement compared to the coupling in quenched QCD is found for  $r \lesssim 0.4$  fm. At distances substantially smaller than 0.1 fm the logarithmic weakening of the coupling enters and will dominate the  $r$ -dependence of  $V(r)$ . The observed running of the coupling may already signal the onset of the short distance perturbative regime. This is also evident from quenched QCD lattice studies of  $V(r)$  [48].

The running coupling at finite temperature defined in the  $qq$ -scheme using the derivative of the color singlet quark anti-quark free energy,  $dF_1(r, T)/dr$ , shows only little qualitative and quantitative differences when changing from pure gauge [20] to full QCD at temperatures well above deconfinement. Again, at small distances the running coupling is controlled by distance and becomes comparable to  $\alpha_{qq}(r)$  at zero temperature. The properties of  $\alpha_{qq}(r, T)$  at temperatures in the vicinity of the phase transition are to large extent controlled by the confinement signal at zero temperature. A clear separation of the different effects usually described by the concepts of color screening ( $T \gtrsim T_c$ ) and the concept of string breaking ( $T \lesssim T_c$ ) is difficult in the crossover region. Remnants of the confinement part of the QCD forces may in parts dominate the non-perturbative properties of the QCD plasma at temperatures only moderately larger than  $T_c$ . This supports similar findings in recent studies of the quark anti-quark free energies in quenched QCD [20].

The properties of the quark anti-quark free energy and the coupling at small distances thus again allow for non-perturbative renormalization of the free energy and Polyakov loop [12]. The crossover from confinement to deconfinement is clearly signaled by the Polyakov loop through a rapid increase at temperatures close to  $T_c$ . String breaking dominates the quark anti-quark free energies at temperatures well below deconfinement in all color channels leading to finite values of the Polyakov loop. The string breaking energy,  $F_\infty(T)$ , and the distance where string breaking sets in, are decreasing with increasing temperatures. The plateau value  $F_\infty(T)$  approaches about 95% of the value one usually estimates at zero temperature,  $V(r_{\text{breaking}}) \simeq 1.1$  GeV [29, 38], already for  $T \simeq 0.8T_c$ . We thus expect that the change in quark anti-quark free energies is only small when going to smaller temperatures and the quark anti-quark free energy,  $F_1(r, T)$ , will show only small differences from the heavy quark potential at  $T = 0$ ,  $V(r)$ . Significant thermal modifications on heavy quark bound states can thus be expected only for temperatures above  $0.8T_c$ . Our analysis of  $r_{\text{med}}$  suggests indeed a qualitative similar behavior for the free energies in 3-flavor QCD. This can also be seen from the behavior of  $r_{\text{med}}$  shown in Fig. 11.

At temperatures well above the (pseudo-) critical temperature, *i.e.*  $1.2 \lesssim T/T_c \lesssim 4$ , no or only little qualitative differences in the thermal properties of the quark anti-quark free energies calculated in quenched

( $N_f=0$ ) and full ( $N_f=2,3$ ) QCD could be established here when converting the observables to physical units. Color screening clearly dominates the quark anti-quark free energy at large distances and screening masses, which are non-perturbatively determined from the exponential fall-off of the color singlet free energies, could be extracted (for  $N_f=2$ ). In accordance with earlier findings in quenched QCD [19, 20] we find substantially larger values for the screening masses than given by leading order perturbation theory. The values of the screening masses,  $m_D(T)$ , again show only marginal differences as function of  $T/T_c$  compared to the values found in quenched QCD (see also Fig. 11). The large screening mass defines a rather small screening radius,  $r_D \equiv 1/m_D$ , which refers to a length scale where the singlet free energy shows almost no deviations from the heavy quark potential at zero temperature. It thus might be misleading to quantify the length scale of the QCD plasma where temperature effects dominate thermal modifications on heavy quark bound states with the observable  $r_D \equiv 1/m_D$  in the non-perturbative temperature regime close but above  $T_c$ . On the other hand the color averaged free energies show indeed strong temperature dependence at distances which could be characterized by  $1/m_D$ . In view of color changing processes as a mechanism for direct quarkonium dissociation [63] the discussion of the color averaged free energy could become important.

We have also compared  $r_D$  and  $r_{\text{med}}$  in Fig. 11 to the expected mean squared charge radii of some charmonium states. It is reasonable that the temperatures at which these radii equal  $r_{\text{med}}$  give a first indication of the temperature at which thermal modifications become important in the charmonium states. It appears thus quite reasonable that  $J/\psi$  will survive the transition while  $\chi_c$  and  $\psi'$  are expected to show strong thermal effects at temperatures in the vicinity of the transition and this may support recent findings [11, 16, 64]. Of course the wave functions of these states will also reach out to larger distances and thus our analysis can only be taken as a first indication of the relevant temperatures. We will turn back to this issue in Ref. [35]. The analysis of bound states using, for instance, the Schrödinger equation will do better in this respect. It can, however, clearly be seen from Fig. 11 that although  $r_{\text{med}}(T_c) \simeq 0.7$  fm is approached almost in common for  $N_f=0,2,3$ , it falls apart for  $N_f=2,3$  at smaller temperatures. It thus could be difficult to determine suppression patterns from free energies for quarkonium states which are substantially larger than 0.7 fm independently from  $N_f$  and/or finite quark mass.

The analysis presented here has been performed for a single quark mass value that corresponds to a pion mass of about 770 MeV ( $m_\pi/m_\rho \simeq 0.7$ ). In Ref. [32], however, no major quark mass effects were visible in color averaged free energies below this quark mass value. The comparisons of  $r_{\text{med}}$  and  $F_\infty(T)$  calculated in 2-flavor ( $m_\pi/m_\rho \simeq 0.7$ ) with results calculated in 3-flavor QCD ( $m_\pi/m_\rho \simeq 0.4$  [33]) supports this property. While at

temperatures above deconfinement no or only little differences in this observable can be identified, at temperatures below  $T_c$  differences can be seen. To what extend these are due to the smaller quark masses used in the 3-flavor case or whether these differences reflect a flavor dependence of the string breaking distance requires further investigation. Despite these uncertainties and the fact that parts of our comparisons to results from quenched QCD are on a qualitative level, we find quite important information for the study of heavy quark bound states in the QCD plasma phase. At temperatures well above  $T_c$ , *i.e.*  $1.2 \lesssim T/T_c \lesssim 4$ , no or only little differences appear between results calculated in quenched and QCD. This might suggest that using thermal parameters extracted from free or internal energy in quenched QCD as input for model calculations of heavy quark bound states [15, 16] is a reasonable approximation. Furthermore this also supports the investigation of heavy quarkonia in quenched lattice QCD calculations using the analysis of spectral functions [10, 11, 65]. On the other hand, however, most of our 2- and 3-flavor QCD results differ from quenched calculations at temperatures in the vicinity and below the phase transition. Due to these qualitative differences, results from quenched QCD could make a discussion of

possible signals for the quark gluon plasma production in heavy ion collision experiments complicated when temperatures and/or densities close to the transition become important.

## Acknowledgments

We thank the Bielefeld-Swansea collaboration for providing us their configurations with special thanks to S. Ejiri. We would like to thank E. Laermann and F. Karsch for many fruitful discussions. F.Z. thanks P. Petreczky for his continuous support. We thank K. Petrov and P. Petreczky for sending us the data of Ref. [34]. This work has partly been supported by DFG under grant FOR 339/2-1 and by BMBF under grant No.06BI102 and partly by contract DE-AC02-98CH10886 with the U.S. Department of Energy. At an early stage of this work F.Z. has been supported through a stipend of the DFG funded graduate school GRK881. Some of the results discussed in this article were already presented in proceeding contributions [23, 66, 67].

---

[1] For recent reviews on lattice results see: E. Laermann and O. Philipsen, Ann. Rev. Nucl. Part. Sci. **53**, 163 (2003) and P. Petreczky, hep-lat/0409139.

[2] L. D. McLerran and B. Svetitsky, Phys. Lett. **B98**, 195 (1981).

[3] L. D. McLerran and B. Svetitsky, Phys. Rev. **D24**, 450 (1981).

[4] T. Matsui and H. Satz, Phys. Lett. **B178**, 416 (1986).

[5] For recent reviews see: N. Brambrilla *et al.*, hep-ph/0412158 and [14].

[6] S. Digal, P. Petreczky, and H. Satz, Phys. Lett. **B514**, 57 (2001).

[7] S. Digal, P. Petreczky, and H. Satz, Phys. Rev. **D64**, 094015 (2001).

[8] C.-Y. Wong, J. Phys. **G28**, 2349 (2002).

[9] C.-Y. Wong, Phys. Rev. **C65**, 034902 (2002).

[10] S. Datta, F. Karsch, P. Petreczky, and I. Wetzorke, Phys. Rev. **D69**, 094507 (2004).

[11] M. Asakawa and T. Hatsuda, Phys. Rev. Lett. **92**, 012001 (2004).

[12] O. Kaczmarek, F. Karsch, P. Petreczky, and F. Zantow, Phys. Lett. **B543**, 41 (2002).

[13] F. Zantow, O. Kaczmarek, F. Karsch, and P. Petreczky, hep-lat/0301015.

[14] F. Karsch, hep-lat/0502014.

[15] E. V. Shuryak and I. Zahed, Phys. Rev. **D70**, 054507 (2004).

[16] C.-Y. Wong, hep-ph/0408020.

[17] G. E. Brown, C.-H. Lee, and M. Rho, Nucl. Phys. **A747**, 530 (2005).

[18] H.-J. Park, C.-H. Lee, and G. E. Brown, hep-ph/0503016.

[19] O. Kaczmarek, F. Karsch, E. Laermann, and M. Lutgemeier, Phys. Rev. **D62**, 034021 (2000).

[20] O. Kaczmarek, F. Karsch, F. Zantow, and P. Petreczky, Phys. Rev. **D70**, 074505 (2004).

[21] B. Beinlich, F. Karsch, E. Laermann, and A. Peikert, Eur. Phys. J. **C6**, 133 (1999).

[22] F. Karsch, E. Laermann, and A. Peikert, Nucl. Phys. **B605**, 579 (2001).

[23] O. Kaczmarek, S. Ejiri, F. Karsch, E. Laermann, and F. Zantow, Prog. Theor. Phys. Suppl. **153**, 287 (2004).

[24] A. Dumitru, J. Lenaghan, and R. D. Pisarski, hep-ph/0410294.

[25] A. Dumitru, Y. Hatta, J. Lenaghan, K. Orginos, and R. D. Pisarski, Phys. Rev. **D70**, 034511 (2004).

[26] C. DeTar, O. Kaczmarek, F. Karsch, and E. Laermann, Phys. Rev. **D59**, 031501 (1999).

[27] O. Kaczmarek, F. Karsch, P. Petreczky, and F. Zantow (2003), hep-lat/0309121.

[28] F. Zantow, Ph.D. thesis, Bielefeld University, Germany (2004).

[29] P. Pennanen and C. Michael (UKQCD), hep-lat/0001015.

[30] C. R. Allton *et al.*, Phys. Rev. **D66**, 074507 (2002).

[31] C. R. Allton *et al.*, Phys. Rev. **D68**, 014507 (2003).

[32] F. Karsch, E. Laermann, and A. Peikert, Phys. Lett. **B478**, 447 (2000).

[33] P. Petreczky, private communication.

[34] P. Petreczky and K. Petrov, Phys. Rev. **D70**, 054503 (2004).

[35] O. Kaczmarek and F. Zantow, to be published.

[36] S. Necco and R. Sommer, Nucl. Phys. **B622**, 328 (2002).

[37] M. Luscher and P. Weisz, JHEP **07**, 049 (2002).

[38] C. W. Bernard *et al.*, Phys. Rev. **D64**, 074509 (2001).

[39] U. Glassner *et al.* (TXL), Phys. Lett. **B383**, 98 (1996).

[40] C. R. Allton *et al.* (UKQCD), Phys. Rev. **D60**, 034507

(1999).

- [41] S. Aoki et al. (CP-PACS), *Nucl. Phys. Proc. Suppl.* **73**, 216 (1999).
- [42] G. S. Bali et al. (TXL), *Phys. Rev.* **D62**, 054503 (2000).
- [43] A. Ali Khan et al. (CP-PACS), *Phys. Rev.* **D65**, 054505 (2002).
- [44] S. Aoki et al. (JLQCD), *Phys. Rev.* **D68**, 054502 (2003).
- [45] G. S. Bali and K. Schilling, *Phys. Rev.* **D47**, 661 (1993).
- [46] M. Peter, *Nucl. Phys.* **B501**, 471 (1997).
- [47] Y. Schroder, *Phys. Lett.* **B447**, 321 (1999).
- [48] S. Necco and R. Sommer, *Phys. Lett.* **B523**, 135 (2001).
- [49] O. Philipsen, *Phys. Lett.* **B535**, 138 (2002).
- [50] S. Nadkarni, *Phys. Rev.* **D34**, 3904 (1986).
- [51] S. Nadkarni, *Phys. Rev.* **D33**, 3738 (1986).
- [52] O. Jahn and O. Philipsen, *Phys. Rev.* **D70**, 074504 (2004).
- [53] M. Gockeler et al., hep-ph/0502212.
- [54] P. de Forcrand and L. von Smekal, *Phys. Rev.* **D66**, 011504 (2002).
- [55] E. Gava and R. Jengo, *Phys. Lett.* **B105**, 285 (1981).
- [56] F. Zantow, hep-lat/0301014.
- [57] N. Attig, F. Karsch, B. Petersson, H. Satz, and M. Wolff, *Phys. Lett.* **B209**, 65 (1988).
- [58] A. Nakamura and T. Saito, *Prog. Theor. Phys.* **111**, 733 (2004).
- [59] M. Laine and Y. Schroder, hep-ph/0503061.
- [60] P. Petreczky et al., *Nucl. Phys.* **A698**, 400 (2002).
- [61] F. Zantow, O. Kaczmarek, F. Karsch, and P. Petreczky, *Nucl. Phys. Proc. Suppl.* **106**, 519 (2002).
- [62] S. Jacobs, M. G. Olsson, and I. Suchyta, Casimir, *Phys. Rev.* **D33**, 3338 (1986).
- [63] D. Kharzeev and H. Satz, *Phys. Lett.* **B334**, 155 (1994).
- [64] P. Petreczky, S. Datta, F. Karsch, and I. Wetzorke, *Nucl. Phys. Proc. Suppl.* **129**, 596 (2004).
- [65] M. Asakawa, T. Hatsuda, and Y. Nakahara, *Nucl. Phys.* **A715**, 863 (2003).
- [66] O. Kaczmarek and F. Zantow, hep-lat/0502011.
- [67] O. Kaczmarek and F. Zantow, hep-lat/0502012.